

**PREPARATION OF NOVEL INORGANIC-ORGANIC HYBRID
MATERIALS BY TEMPLATE-DIRECTED SYNTHESIS USING
BACTERIAL CELLULOSE AS A MATRIX**

Chaiyapruk Katepetch

A Dissertation Submitted in Partial Fulfilment of the Requirements
for the Degree of Doctor of Philosophy
The Petroleum and Petrochemical College, Chulalongkorn University
in Academic Partnership with
The University of Michigan, The University of Oklahoma,
and Case Western Reserve University

2013

I28372955

561 054

Thesis Title: Preparation of Novel Inorganic-Organic Hybrid Materials by Template-Directed Synthesis Using Bacterial Cellulose as a Matrix

By: Chaiyapruk Katepetch

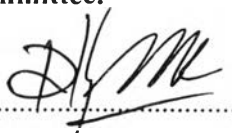
Program: Polymer Science

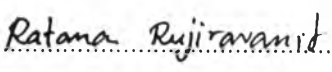
Thesis Advisors: Assoc. Prof. Ratana Rujiravanit (*Thai Advisor*)
Prof. Hiroshi Tamura (*Overseas Advisor*)


Accepted by The Petroleum and Petrochemical College, Chulalongkorn University, in partial fulfilment of the requirements for the Degree of Doctor of Philosophy.

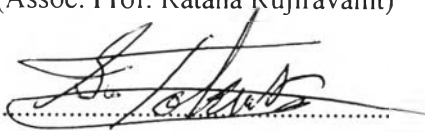

..... College Dean
(Asst. Prof. Pomthong Malakul)


Thesis Committee:

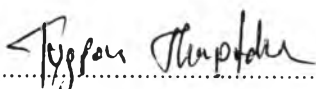

.....
(Asst. Prof. Pomthong Malakul)


.....
(Assoc. Prof. Ratana Rujiravanit)


.....
(Prof. Hiroshi Tamura)


.....
(Prof. Seiichi Tokura)


.....
(Prof. Anuvat Sirivat)


.....
(Dr. Tuspon Thanpitcha)

ABSTRACT

5092002063: Polymer Science Program

Student's Name: Chaiyapruk Katepetch

Thesis Title: Preparation of Novel Inorganic-Organic Hybrid Materials by Template-Directed Synthesis Using Bacterial Cellulose as a Matrix

Thesis Advisors: Assoc Prof. Ratana Rujiravanit (*Thai Advisor*) and Prof. Hiroshi Tamura (*Overseas Advisor*).

Keywords: Inorganic-Organic Hybrid Materials/ Bacterial Cellulose/ Magnetic Particles/ Silver Particles/ Zinc Oxide Particles

In the present study, the novel inorganic–organic hybrid materials of magnetic particles, silver particles, zinc oxide particles and bacterial cellulose (BC) were successfully prepared by using template-directed synthesis method. The cations precursor of magnetic, silver and zinc oxide particles were firstly homogeneously dispersed into the BC matrix. Then, the dispersed-cations were converted to be metal or metal oxide particles inside BC matrix. By using BC as a template, the homogeneously distribution with optimizing particle size of the as-synthesized metal and metal oxide particles inside BC matrix were successfully achieved. These were resulted in the synergistic properties between the as-synthesized metal or metal oxide particles and BC matrix. The as-prepared samples were investigated by scanning electron microscope (SEM), transmission electron microscope (TEM), energy dispersive X-ray (EDX), X-ray diffraction (XRD) techniques and thermogravimetric analysis (TGA). The magnetic and electric properties of the as-prepared magnetic particle, silver particle and magnetic/silver particle incorporated-BC samples were studied by using the vibrating sample magnetometry (VSM) and two points probe conductivity meter, respectively. Finally, the photo-catalytic activities of the as-prepared zinc oxide particle incorporated-bacterial cellulose samples were studied by monitoring the antibacterial activity of the as-prepared sample.

บทคัดย่อ

ชื่อ ชัยพฤกษ์ นามสกุล เกตุเพชร : ชื่อหัวข้อวิทยานิพนธ์ (ภาษาไทย) การเตรียมวัสดุ
 ลูกผสมระหว่างสาร อนินทรีย์และสารอินทรีย์ชนิดใหม่ผ่านกระบวนการการสังเคราะห์โดยใช้เส้น
 ใยแบคทีเรียเซลลูโลสเป็นโครงร่าง (ภาษาอังกฤษ) (Preparation of Novel Inorganic-Organic
 Hybrid Materials by Template-Directed Synthesis Using Bacterial Cellulose as a
 Matrix) อ. ที่ปรึกษา : รศ. รัตนา รุจิรวนิช และ ศ. อิโรชิ ทามูระ 181 หน้า

ในงานวิจัยนี้ ได้ประสบความสำเร็จในการเตรียมวัสดุลูกผสมระหว่างสารอนินทรีย์และ
 สารอินทรีย์ ที่ประกอบด้วย อนุภาคแม่เหล็ก อนุภาคเงิน อนุภาคซิงค์ออกไซด์ และ เส้นใย
 เซลลูโลส ซึ่งเตรียมผ่านกระบวนการ การสังเคราะห์โดยใช้เส้นใยแบคทีเรียเซลลูโลสเป็นโครงร่าง
 โดยที่ สารตั้งต้นในการสังเคราะห์ อนุภาคแม่เหล็ก อนุภาคเงิน และ อนุภาคซิงค์ ออกไซด์ ซึ่งอยู่
 ในรูปของไอออนบวก จะถูกดูดซับและกระจายตัวอย่างสม่ำเสมอในเมตริกซ์ของเส้นใยแบคทีเรีย
 เซลลูโลสหลังจากนั้นสารตั้งต้นดังกล่าวจะถูกเปลี่ยนเป็นอนุภาคแม่เหล็ก อนุภาคเงิน อนุภาคซิงค์
 ออกไซด์และตกตะกอนอยู่ในเมตริกซ์ของเส้นใยแบคทีเรียเซลลูโลส ซึ่งการใช้กระบวนการเตรียม
 ดังกล่าวร่วมกับเส้นใยแบคทีเรียเซลลูโลสเป็นเมตริกซ์ สามารถเห็นยวนำให้เกิดอนุภาคโลหะ และ
 อนุภาคโลหะออกไซด์ ที่มีขนาดอนุภาคที่เหมาะสมและมีการกระจายตัวอย่างสม่ำเสมอตลอดทั้ง
 เมตริกซ์ได้ โดยสมบัติของวัสดุลูกผสมที่เตรียมได้นั้นจะสามารถวิเคราะห์ได้โดยเทคนิคดังต่อไปนี้
 Scanning electron microscope (SEM) transmission electron microscope (TEM)
 energy dispersive X-ray (EDX) X-ray diffraction (XRD) และ thermo gravimetric
 analysis (TGA) โดยที่ สมบัติทางแม่เหล็กและสมบัติทางไฟฟ้าของ เส้นใยแบคทีเรียเซลลูโลสที่
 ประกอบด้วยอนุภาคแม่เหล็ก เส้นใยแบคทีเรียเซลลูโลสที่ประกอบด้วยอนุภาคเงิน และ เส้นใย
 แบคทีเรียเซลลูโลสที่ประกอบด้วยทั้งอนุภาคแม่เหล็กและอนุภาคเงิน สามารถวิเคราะห์ได้โดย
 เทคนิค vibrating sample magnetometry (VSM) และ two points probe conductivity
 meter ตามลำดับ นอกจากนี้ สมบัติ photocatalytic activities ของ เส้นใยแบคทีเรียเซลลูโลส
 ที่ประกอบด้วยอนุภาคซิงค์ ออกไซด์ สามารถศึกษาได้ ผ่านการศึกษาฤทธิ์ในการต้านเชื้อแบคทีเรีย
 ของตัวอย่างใยแบคทีเรียเซลลูโลสที่ประกอบด้วยอนุภาคซิงค์ ออกไซด์ที่เตรียมได้

ACKNOWLEDGEMENTS

This work is greatly supported in cash and in kind by the Chulalongkorn University Dutsadi Phiphat Scholarship, the Rachadapisek Somphot Endowment Fund, The Petroleum and Petrochemical College, Chulalongkorn University, Thailand, The Conductive and Electroactive Polymers Research Unit and Kansai University, are greatly acknowledged.

This thesis work is funded by the Petroleum and Petrochemical College; and Center of Excellence on Petrochemical and Materials Technology, Thailand.

TABLE OF CONTENTS

	PAGE
Title Page	i
Abstract (in English)	ii
Abstract (in Thai)	iii
Acknowledgements	iv
Table of Contents	v
List of Tables	viii
List of Figures	x
 CHAPTER	
I INTRODUCTION	1
 II LITERATURE REVIEW	 6
 III SYNTHESIS OF MAGNETIC NANOPARTICLE INTO BACTERIAL CELLULOSE MATRIX BY AMMONIA GAS-ENHANCEING <i>IN SITU</i> CO-PRECIPIATION	
METHOD	20
3.1 Abstract	20
3.2 Introduction	20
3.3 Experimental	24
3.4 Results and Discussion	27
3.5 Conclusions	40
3.6 Acknowledgements	41
3.7 References	41

CHAPTER		PAGE
IV	PREPARATION OF ELECTRICALLY CONDUCTIVE CELLULOSE BY AMMONIA GAS-ENHANCEING <i>IN SITU</i> SYNTHESIS OF SILVER PARTICLES INTO BACTERIAL CELLULOSE MATRIX	
	4.1 Abstract	46
	4.2 Introduction	47
	4.3 Experimental	51
	4.4 Results and Discussion	54
	4.5 Conclusions	68
	4.6 Acknowledgements	70
	4.7 References	71
V	PREPARATION OF CELLULOSE SHEETS CONTAINING SILVER/MAGNETIC PARTICLES FOR MAGNETICALLY AND ELECTRICALLY RESPONSIVE MATERIAL APPLICATION	
	5.1 Abstract	75
	5.2 Introduction	76
	5.3 Experimental	80
	5.4 Results and Discussion	84
	5.5 Conclusions	99
	5.6 Acknowledgements	102
	5.7 References	102

CHAPTER	PAGE
VI	
FORMATION OF NANOCRYSTALLINE ZnO ON NANOFIBRIALS OF BACTERIAL CELLULOSE PELLICLE BY IN SITU SYNTHESIS UNDER ULTRASONIC TREATMENT	106
6.1 Abstract	106
6.2 Introduction	107
6.3 Experimental	110
6.4 Results and Discussion	114
6.5 Conclusions	128
6.6 Acknowledgements	130
6.7 References	130
VII	
CONCLUSIONS AND RECOMMENDATIONS	135
REFERENCES (if any)	137
APPENDIX (or APPENDICES)	144
Appendix A	144
Appendix B	164
Appendix C	176
Appendix D	177
CURRICULUM VITAE	179

LIST OF TABLES

TABLE		PAGE
CHAPTER II		
2.1	Bacterial cellulose producers and feature of their product	8
2.2	Physical and magnetic properties of iron oxides	13
CHAPTER III		
3.1	The percent incorporation of magnetic particle, weight percent of iron content and displacement responding to the magnetic field of magnetic particle-incorporated bacterial cellulose sheet prepared by ammonia gas-enhanced <i>in situ</i> co-precipitation method using 0.1 M, 0.05 M, and 0.01 M aqueous iron ion solution	40
CHAPTER V		
5.1	Magnetic and electric properties of magnetic particle incorporated-BC sample prepared by using 0.50 M of aqueous iron ion solution (a) and magnetic and silver particle incorporated-BC samples prepared by using 0.50 M of aqueous iron ion solution and followed by using 0.01 M (b), 0.05 M (c) and 0.10 M (d) of silver nitrate solution, respectively.	101

TABLE	PAGE
CHAPTER VI	
6.1 Crystalline size and percent incorporation of ZnO particle inside the as-prepared ZnO particle incorporated-BC at various preparation conditions	123
6.2 Colony forming unit counts (CFU/ml) at 0h and 24h contact time intervals with the as-prepared ZnO particle incorporated-BC against <i>S. aureus</i> and <i>E. coli</i> .	127

LIST OF FIGURES

FIGURE		PAGE
CHAPTER II		
2.1	Chemical structure of bacterial cellulose.	6
2.2	Pathways for synthesizing of cellulose.	7
2.3	Pathways of carbon metabolism in <i>Acetobacter Xylinum</i> .	9
2.4	Formation of bacterial cellulose ribbon.	10
2.5	SEM image of the bacterial cellulose ribbon produced by a bacterial cell (a) and the bacterial cellulose network including the bacterial cells (b).	10
2.6	Bacterial cellulose in the form of pellicle (a) and irregular granules (b).	11
2.7	Alignment of individual atomic magnetic moments in different types of materials.	13
2.8	Magnetic domains in a bulk material.	14
2.9	Magnetization M as a function of an applied magnetic field H.	15
2.10	Plasmon oscillation of the free electron on the surface of metal nanoparticle.	17
2.11	Mechanism of particle-induced reactive-oxygen-species (ROS).	19
CHAPTER III		
3.1	Schematic diagram of the laboratory set up for preparation of the magnetic particle-incorporated bacterial cellulose pellicle by ammonia gas-enhanced <i>in situ</i> co-precipitation method.	30

FIGURE	PAGE
3.2	
Magnetic particle-incorporated bacterial cellulose pellicles prepared by stepwise dipping process using 0.01 M (a), 0.05 M (b) and 0.1 M (c) of aqueous iron ion solutions and magnetic particle-incorporated bacterial cellulose pellicles prepared by ammonia gas-enhancing <i>in situ</i> co-precipitation method using 0.01 M (d), 0.05 M (e) and 0.1 M (f) of aqueous iron ion solutions.	31
3.3	
XRD pattern of magnetic particle-incorporated bacterial cellulose sheet, prepared by ammonia gas-enhanced <i>in situ</i> co-precipitation method operated in a closed system without oxygen using 0.1 M of aqueous iron ion solution. SEM image of the bacterial cellulose ribbon produced by a bacterial cell (a) and the bacterial cellulose network including the bacterial cells (b).	31
3.4	
SEM images of surface (a) and cross-sectional (b) morphology of neat bacterial cellulose at a magnification of 10,000x and SEM images of surface (c) and cross-sectional (d) morphology of magnetic particle-incorporated bacterial cellulose sheet prepared by ammonia gas-enhanced <i>in situ</i> co-precipitation method using 0.1 M of aqueous iron ion solution at a magnification of 10,000x. Alignment of individual atomic magnetic moments in different types of materials.	33

FIGURE	PAGE
3.5 TEM images and histograms of magnetic particle-incorporated bacterial cellulose sheet prepared by ammonia gas-enhanced <i>in situ</i> co-precipitation method using 0.1 M (a and b), 0.05 M (c and d), and 0.01 M (e and f) of aqueous iron ion solutions.	34
3.6 TEM image of cross-sectional magnetic particle-incorporated bacterial cellulose sheet at a magnification of 2,500×.	34
3.7 Magnetic hysteresis loop of magnetic particle-incorporated bacterial cellulose sheet at the temperature of 300 K (a) and 100 K (b) and magnified view of its hysteresis loop at the temperature of 300 K (c) and 100 K (d).	38

CHAPTER IV

4.1 The experimental set up for preparing of the Ag nanoparticle incorporated-BC by using the ammonia gas enhanced- <i>in situ</i> synthesis method.	54
4.2 Surface and cross-sectional morphology of pristine BC at the magnification of 10,000× (a) and 1,500× (b), respectively.	57
4.3 The UV-Vis absorption spectra of the as-prepared Ag particle incorporated -BC prepared from the Ag ⁺ : glucose molar ratio of 1:10, 1:100 and 1:1000.	57
4.4 TEM images and histograms of the as-prepared Ag particle-incorporated BC samples prepared by ammonia gas-enhanced <i>in situ</i> synthesis with the mole ratio of Ag ⁺ : glucose was 1:10 (a and d), 1:100 (b and e) and 1:1000 (c and f), respectively.	58

FIGURE	PAGE	
4.5	The surface morphology of the pristine BC (a) and the as-prepared Ag particle-incorporated BC samples prepared by ammonia gas-enhanced <i>in situ</i> synthesis, the concentration of AgNO ₃ in the precursor solution were varied to be 0.010 (b), 0.025(c), 0.050(d), 0.075(e) and 0.100 M, respectively.	60
4.6	X-ray diffraction spectra of pristine BC (a) and the as-prepared Ag particle-incorporated BC sample prepared by ammonia gas-enhancing <i>in situ</i> synthesis method with using precursor solution of 0.010 (b), 0.025 (c), 0.050 (d), 0.075 (e) and 0.100 M (f), respectively; the mole ratio of Ag ⁺ : glucose in the precursor solution was fixed at 1:10. Magnetic hysteresis loop of magnetic particle-incorporated bacterial cellulose sheet at the temperature of 300 K (a) and 100 K (b) and magnified view of its hysteresis loop at the temperature of 300 K (c) and 100 K (d).	60
4.7	TGA thermograms of pristine BC (a) and compared to the Ag particle incorporated-BC which were prepared by ammonia gas-enhancing <i>in situ</i> synthesis method with 0.010 (b), 0.025 (c), 0.050 (d), 0.075 (e) and 0.100 M (f) of AgNO ₃ , respectively and the mole ratio of Ag ⁺ : glucose was fixed at 1:10. Inset showed the percent incorporation of Ag particle in the as-prepared Ag particle incorporated-BC sample with increasing of the Ag ⁺ concentration in precursor solution. The percent incorporation of Ag particle is the difference in weight loss when compared to the pristine BC.	64

FIGURE	PAGE
4.8 The electrical conductivity of pristine BC and the as-prepared Ag particle-incorporated BC sample prepared by ammonia gas-enhancing <i>in situ</i> synthesis method with using precursor solution of 0.010, 0.025, 0.050, 0.075 and 0.100 M, respectively; the mole ratio of Ag ⁺ : glucose in the precursor solution was fixed at 1:10.	67

CHAPTER V

5.1 Schematic diagram of the laboratory set up for preparation of the magnetic particle-incorporated bacterial cellulose pellicle by ammonia gas-enhanced <i>in situ</i> co-precipitation method.	82
5.2 Surface and cross-sectional morphology of neat BC at the magnification of 10,000× (a) and 1,500× (b), respectively.	85
5.3 SEM images of magnetic particle-incorporated BC samples, prepared by ammonia gas-enhancing <i>in situ</i> co-precipitation method with 0.01 M (figure 5.3a), 0.05 M (figure 5.3b), 0.1 M (figure 5.3c), 0.5 M (figure 5.3d) and 1 M (figure 5.3e) of aqueous iron ion solution, at the magnification of 40,000×.	88
5.4 TGA thermograms of Neat BC (a) and magnetic particle incorporated-BC samples prepared by ammonia gas-enhancing <i>in situ</i> co-precipitation method using 0.01 M (b), 0.05 M (c), 0.10 M (d), 0.50 M (e) and 1.00 M (f) aqueous iron ion solutions. Inset showed the percent incorporation of magnetic particle in the magnetic particle incorporated-BC sample with increasing of the aqueous iron ion concentration. The percent incorporation of magnetic particle is the difference in weight loss when compared to the neat BC.	88

FIGURE	PAGE	
5.5	Magnetic hysteresis loop of magnetic particle incorporated-BC sample at the temperature of 300 K (a) and magnified view of its hysteresis loop (b).	90
5.6	The XRD patterns of neat BC (a), magnetic particle incorporated-BC sample prepared by using 0.50 M of aqueous iron ion solution (b), silver particle incorporated-BC sample prepared by using 0.10 M of silver nitrate solution (c) and magnetic and silver particle incorporated-BC BC sample prepared by using 0.50 M of aqueous iron ion solution and followed by using 0.10 M of silver nitrate solution (d).	94
5.7	TGA thermograms of the magnetic and silver particle incorporated-BC samples prepared by sodium borohydride-enhancing <i>in situ</i> synthesis method with using 0.01 M, 0.05 M and 0.10 M of silver nitrate solution, respectively. Inset showed the percent remaining residue of magnetic and silver particle in the magnetic particle incorporated-BC in comparing with the as-prepared magnetic particle incorporated-BC sample.	95
5.8	Magnetic hysteresis loop of silver particle incorporated-BC sample prepared by using 0.10 M of silver nitrate solution, magnetic particle incorporated-BC sample prepared by using 0.50 M of aqueous iron ion solution and magnetic and silver particle incorporated-BC sample prepared by using 0.50 M of aqueous iron ion solution and followed by using 0.01 M, 0.05 M and 0.10 M of silver nitrate solution, respectively.	98

FIGURE	PAGE
CHAPTER VI	
6.1 Schematic diagram of the experimental set-up for preparing of ZnO particle incorporated-BC by ultrasonic assisted- <i>in situ</i> synthesis method.	115
6.2 SEM images of surface and cross-sectional morphology of neat BC at magnification of 5,000× (a) and 1500× (b), respectively, SEM images of surface morphology of ZnO particle incorporated-BC prepared by the ultrasonic-assisted synthesis method with 6 h of immersion in zinc acetate solution and followed by 1 h of ultrasonic treatment at magnification of 650× (c) and 5,000× (d), respectively and X-ray dot mapping images for surface morphology of zinc elemental of ZnO particle incorporated-BC at magnification of 650× (e) and 5000× (f).	117
6.3 X-ray diffraction spectra of ZnO particle-incorporated BC prepared by ultrasonic-assisted synthesis method with 6h (a), 3h (b) and 1h (c) immersing in zinc acetate solution and followed by 1h ultrasonic treatment.	120
6.4 TGA thermograms of neat BC (BC) compared to that of nanocrystalline ZnO particle incorporated-BC were prepared by immersing of BC pellicle in zinc acetate solution for 1h (ZnO-BC/1/1), 3h (ZnO-BC/3/1) and 6h (ZnO-BC/6/1). Then, followed by 1h of ultrasonic treatment time (a) and TGA thermograms of neat BC (BC) compared to nanocrystalline ZnO particle incorporated-BC prepared by immersing of BC pellicle in zinc acetate solution for 3 h and followed by 0.5h (ZnO-BC/3/0.5), 1h (ZnO-BC/3/1) and 2h (ZnO-BC/3/2) of ultrasonic treatment time (b).	122

FIGURE	PAGE
6.5 Antibacterial activity of as-prepared ZnO particle incorporated-BC sample with 37.32 ± 0.61 %wt of ZnO against (a) <i>S. aureus</i> and (b) <i>E. coli</i> .	124